



# Rediscovery of “wrong-sign” $D^0$ decays to hadronic final states with early Belle II data

The Belle II collaboration

In the standard model, mixing and  $CP$  violation in the charm sector are expected to be very small and thus they constitute a sensitive probe for potential new physics contributions. The “wrong-sign”(WS) decays  $D^{*+} \rightarrow D^0\pi^+$  with  $D^0 \rightarrow K^+\pi^-, K^+\pi^-\pi^0, K^+\pi^-\pi^+\pi^-$  are among the best channels to study charm mixing, as they can be produced through two interfering processes: a direct doubly Cabibbo-suppressed decay of the  $D^0$  meson, or through  $D^0-\bar{D}^0$  mixing followed by a Cabibbo-favored decay of the  $\bar{D}^0$  meson. The “right-sign” (RS) decays  $D^{*+} \rightarrow D^0\pi^+$  with  $D^0 \rightarrow K^-\pi^+, K^-\pi^+\pi^0, K^-\pi^+\pi^+\pi^-$ , which are dominated by the Cabibbo-favored decay and hence not sensitive to mixing, serve as a normalization. This note reports the “rediscovery” of the three WS decays and the measurement of the WS-to-RS ratios in the data collected by Belle II during 2019 and the first half of 2020, and corresponding to  $37.8 \text{ fb}^{-1}$  of integrated luminosity.

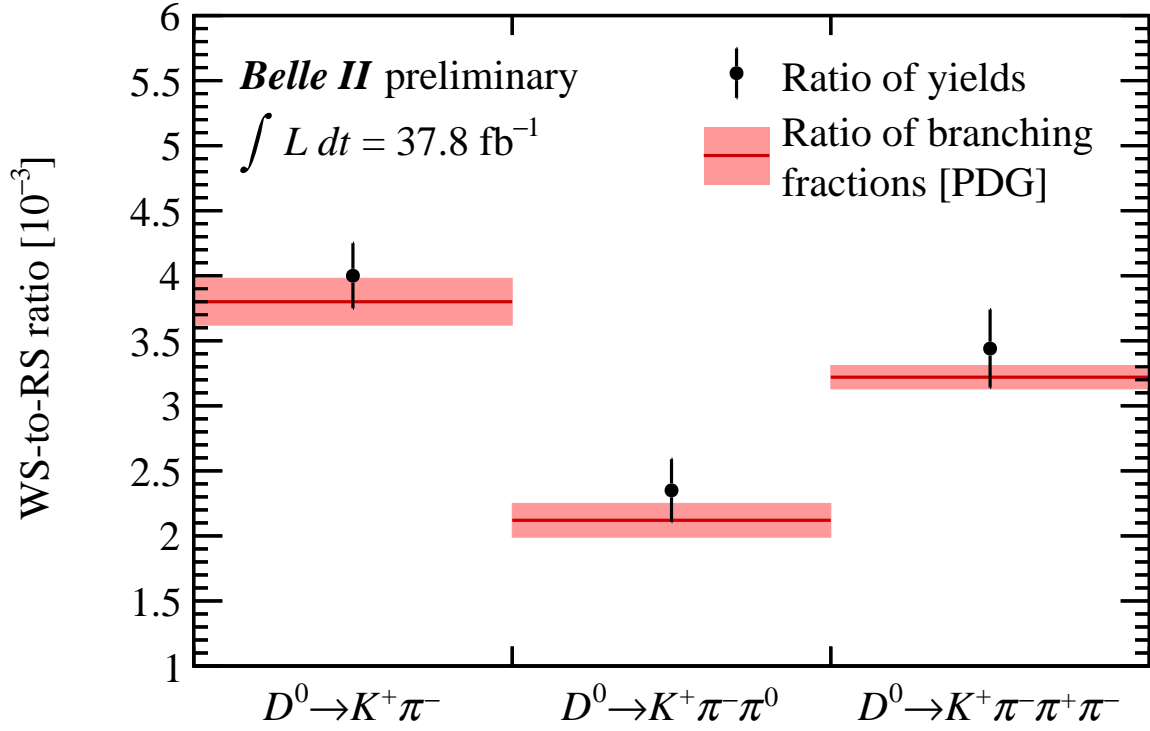


Figure 1: Measured ratios (with statistical-only uncertainties) of wrong-sign (WS) to right-sign (RS) decay yields using data collected by Belle II during 2019 and the first half of 2020, and corresponding to an integrated luminosity of  $37.8 \text{ fb}^{-1}$ , in comparison with the corresponding world-average ratios of branching fractions from the PDG. For each decay mode, the wrong-sign (WS) and right-sign (RS) efficiencies are assumed to be the same.

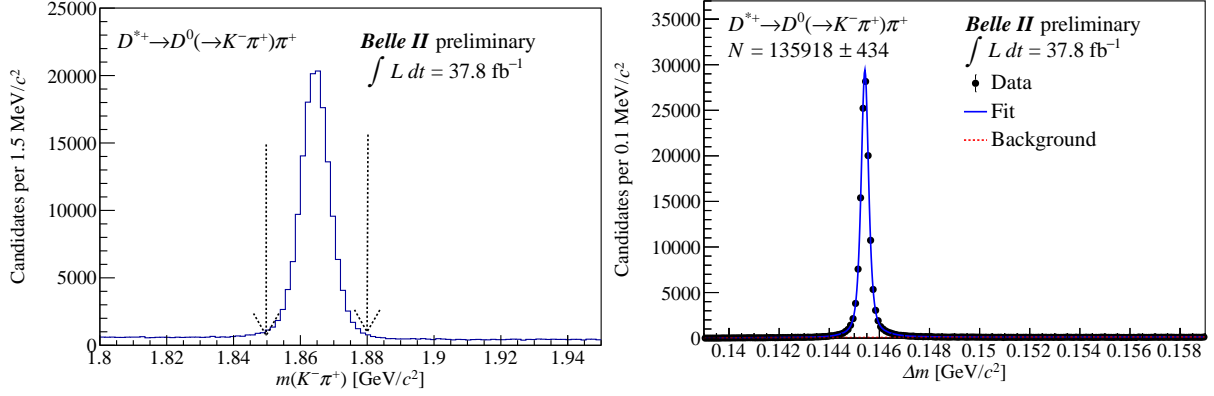


Figure 2: Distribution of (left)  $m(K^-\pi^+)$  and (right) difference of  $m(K^-\pi^+\pi^+)$  and  $m(K^-\pi^+)$  [ $\Delta m$ ] for right-sign (RS)  $D^0 \rightarrow K^-\pi^+$  candidates reconstructed in data collected by Belle II during 2019 and the first half of 2020, and corresponding to an integrated luminosity of  $37.8 \text{ fb}^{-1}$ . The  $\Delta m$  distribution is only for candidates populating the  $D^0$ -mass signal region, indicated by the vertical lines, and after the removal of the multiple  $D^{*+}$  candidates.

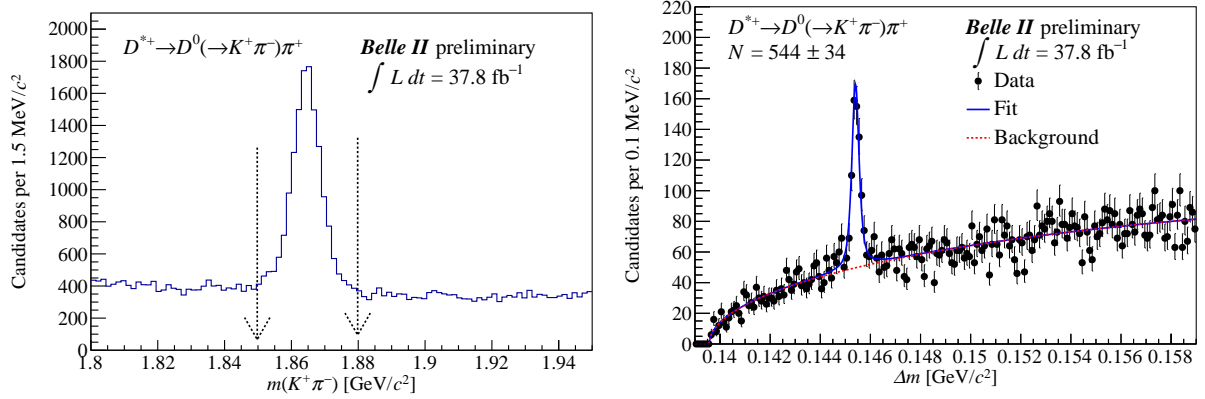


Figure 3: Distribution of (left)  $m(K^+\pi^-)$  and (right) difference of  $m(K^+\pi^-\pi^+)$  and  $m(K^+\pi^-)$  [ $\Delta m$ ] for wrong-sign (WS)  $D^0 \rightarrow K^+\pi^-$  candidates reconstructed in data collected by Belle II during 2019 and the first half of 2020, and corresponding to an integrated luminosity of  $37.8 \text{ fb}^{-1}$ . The  $\Delta m$  distribution is only for candidates populating the  $D^0$ -mass signal region, indicated by the vertical lines, and after the removal of the multiple  $D^{*+}$  candidates.

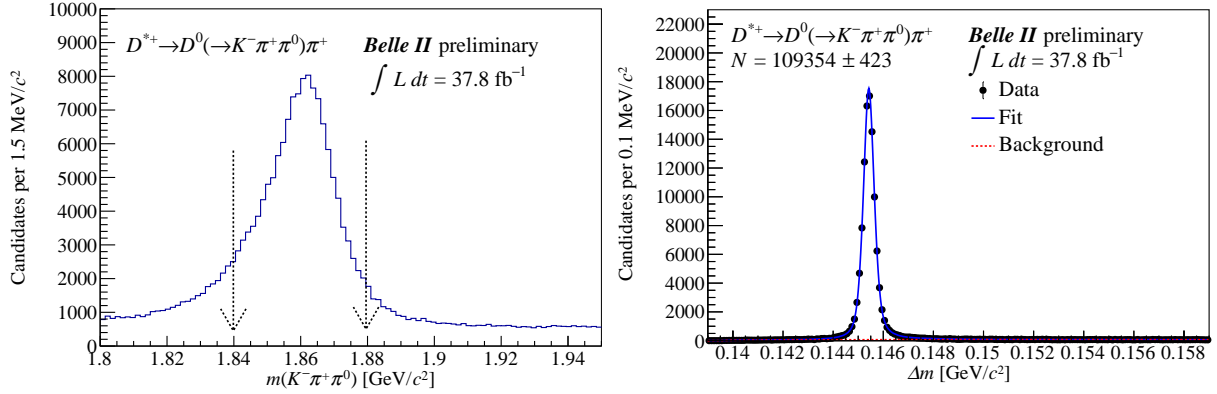


Figure 4: Distribution of (left)  $m(K^-\pi^+\pi^0)$  and (right) difference of  $m(K^-\pi^+\pi^0\pi^+)$  and  $m(K^-\pi^+\pi^0)$  [ $\Delta m$ ] for right-sign (RS)  $D^0 \rightarrow K^-\pi^+\pi^0$  candidates reconstructed in data collected by Belle II during 2019 and the first half of 2020, and corresponding to an integrated luminosity of  $37.8 \text{ fb}^{-1}$ . The  $\Delta m$  distribution is only for candidates populating the  $D^0$ -mass signal region, indicated by the vertical lines, and after the removal of the multiple  $D^{*+}$  candidates.

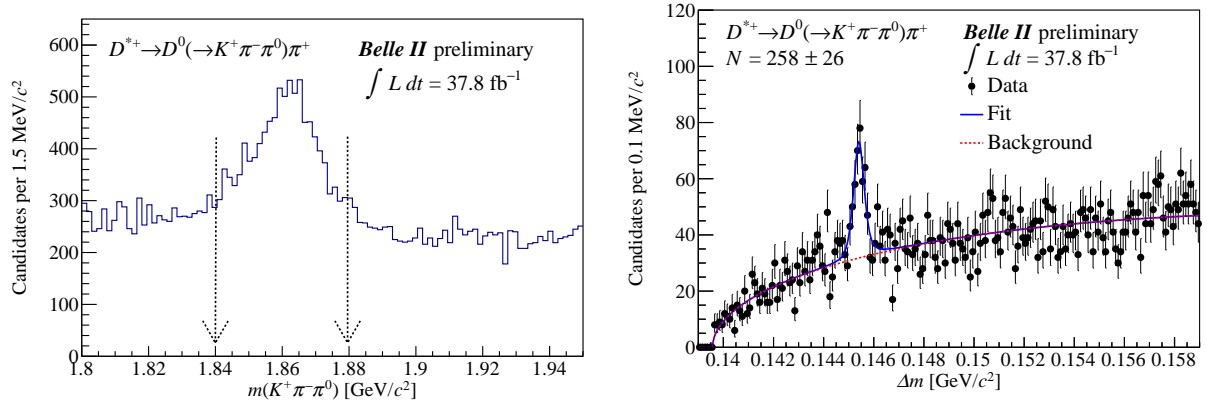


Figure 5: Distribution of (left)  $m(K^+\pi^-\pi^0)$  and (right) difference of  $m(K^+\pi^-\pi^0\pi^+)$  and  $m(K^+\pi^-\pi^0)$  [ $\Delta m$ ] for wrong-sign (WS)  $D^0 \rightarrow K^+\pi^-\pi^0$  candidates reconstructed in data collected by Belle II during 2019 and the first half of 2020, and corresponding to an integrated luminosity of  $37.8 \text{ fb}^{-1}$ . The  $\Delta m$  distribution is only for candidates populating the  $D^0$ -mass signal region, indicated by the vertical lines, and after the removal of the multiple  $D^{*+}$  candidates.

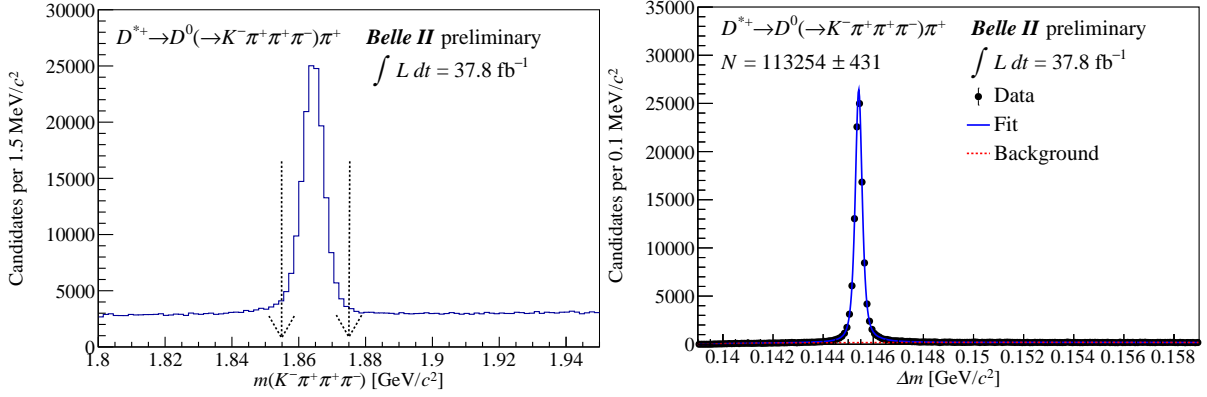


Figure 6: Distribution of (left)  $m(K^- \pi^+ \pi^+ \pi^-)$  and (right) difference of  $m(K^- \pi^+ \pi^+ \pi^-)$  and  $m(K^- \pi^+ \pi^+ \pi^-)$  [ $\Delta m$ ] for right-sign (RS)  $D^0 \rightarrow K^- \pi^+ \pi^+ \pi^-$  candidates reconstructed in data collected by Belle II during 2019 and the first half of 2020, and corresponding to an integrated luminosity of  $37.8 \text{ fb}^{-1}$ . The  $\Delta m$  distribution is only for candidates populating the  $D^0$ -mass signal region, indicated by the vertical lines, and after the removal of the multiple  $D^{*+}$  candidates.

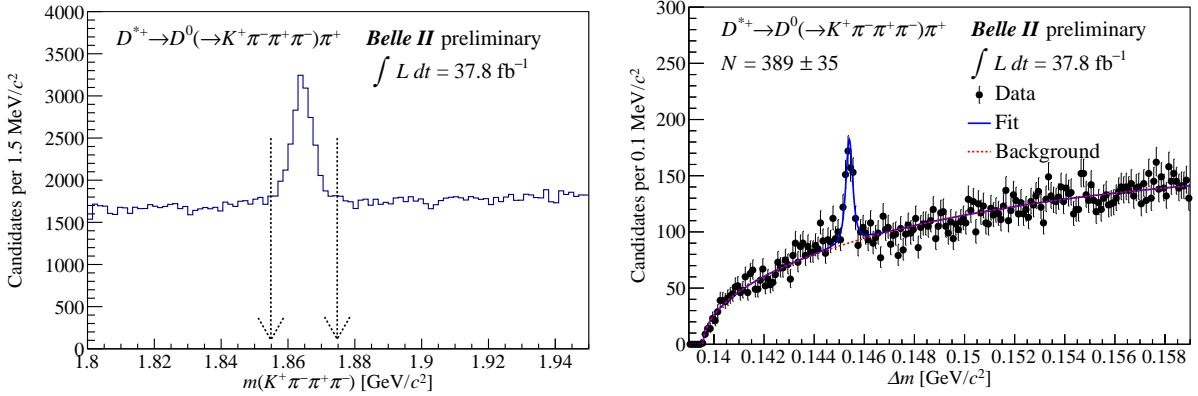


Figure 7: Distribution of (left)  $m(K^+ \pi^- \pi^+ \pi^-)$  and (right) difference of  $m(K^+ \pi^- \pi^+ \pi^-)$  and  $m(K^+ \pi^- \pi^+ \pi^-)$  [ $\Delta m$ ] for wrong-sign (WS)  $D^0 \rightarrow K^+ \pi^- \pi^+ \pi^-$  candidates reconstructed in data collected by Belle II during 2019 and the first half of 2020, and corresponding to an integrated luminosity of  $37.8 \text{ fb}^{-1}$ . The  $\Delta m$  distribution is only for candidates populating the  $D^0$ -mass signal region, indicated by the vertical lines, and after the removal of the multiple  $D^{*+}$  candidates.